

Abstract

The platform motions of floating offshore wind turbines generate unsteady wake dynamics that influence downstream power production and fatigue loading. Accurate modelling of floating wind farms therefore requires improved understanding of these motion-induced wake dynamics. However, the aerodynamic effects of the tower and nacelle are often neglected in numerical simulations. This study aims to:

- (i) **Assess the influence of the tower and nacelle on wake dynamics under different platform motions**
- (ii) **Evaluate lower-fidelity meshless methods as an alternative to dynamic meshing**

Results show that although blade-scale tower-nacelle effects are not fully resolved by lower-fidelity approaches, the dominant platform-induced wake dynamics are captured accurately. The influence of the tower and nacelle on wake coherence depends on the platform degree of freedom: for the conditions studied, their inclusion enhances wake meandering for roll motion, while pitch-induced wake dynamics remain largely unchanged.

Case Examples

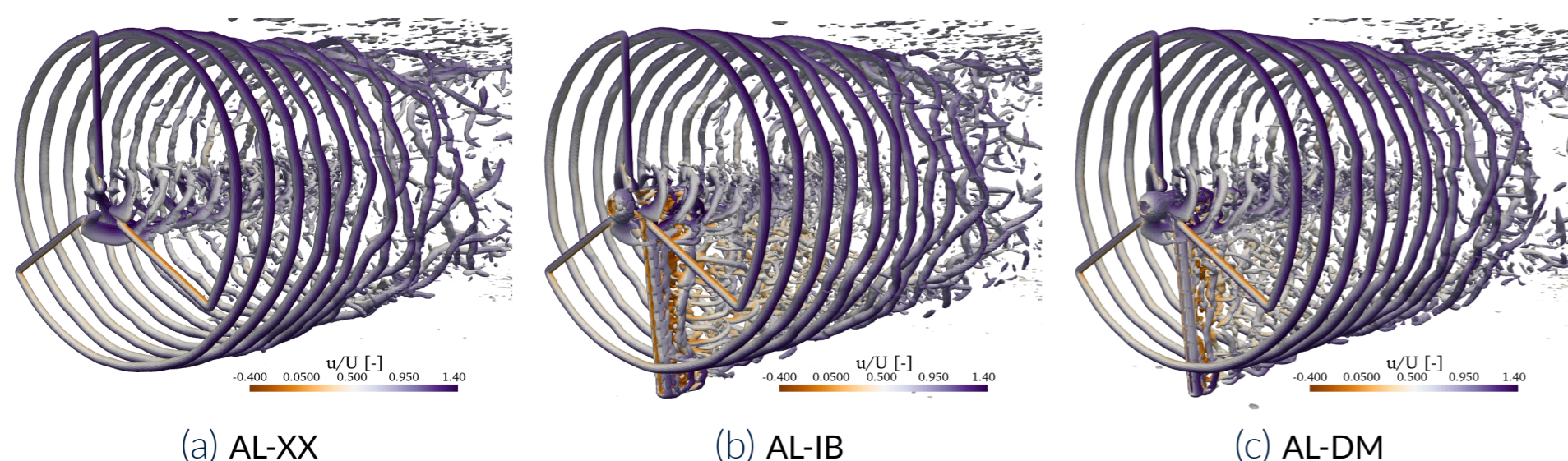


Figure 1. Instantaneous snapshots of the wake showing Q -criterion contours coloured by the normalised streamwise velocity u_x/U_∞ for a rolling turbine with $(f_p^*, A_p) = (0.30, 1.9^\circ)$.

Methodology

- ▶ Numerical setup reproduces the NETTUNO wind tunnel experiment [2]
- ▶ Wind tunnel boundary layers modelled using a wall-modelled approach
- ▶ Prescribed sinusoidal platform turbine motions with non-dimensional frequency, $f_p^* = f_p D/U_\infty$, and amplitude, A_p , defining non-dimensional platform time $\tau = f_p t$
- ▶ Inflow turbulence generated using the divergence-free synthetic eddy method [3]
- ▶ LES with WALE subgrid-scale model for turbulence closure
- ▶ Turbine blades modelled using an Actuator Line Model (ALM)
- ▶ Potential-flow velocity sampling for force evaluation [4]
- ▶ Two tower-nacelle representations compared...

Immersed Boundary Method (IBM)

The immersed boundary method is implemented using a Brinkman penalisation approach. Solid motion is imposed through a body force added to the momentum equations,

$$\mathbf{f} = \chi_s \lambda (\mathbf{u} - \mathbf{u}_s),$$

where $\chi_s \in [0, 1]$ is a mask function defining the immersed solid region, \mathbf{u} is the fluid velocity, \mathbf{u}_s is the prescribed solid velocity, and λ is a penalisation factor. The value of λ is selected to enforce the solid motion accurately while avoiding excessive numerical stiffness.

Dynamic Mesh Method (DMM)

The dynamic motion is represented by deforming the computational mesh in response to prescribed structural motion. Mesh displacement is obtained solving

$$\nabla \cdot (\gamma \nabla \mathbf{d}) = 0,$$

where \mathbf{d} is the mesh displacement vector and γ is a diffusivity defined as the inverse of the distance to the moving body, ensuring smooth deformation away from solid boundaries. The resulting displacement field is then used to update the mesh. Near-wall flow is modelled using a wall model.

Case Keys

- ▶ **AL-XX**: ALM blades + no tower/nacelle
- ▶ **AL-IB**: ALM blades + IBM tower/nacelle
- ▶ **AL-DM**: ALM blades + DMM tower/nacelle
- ▶ **BR-DM**: Resolved blades + DMM tower/nacelle [1]
- ▶ **EXP**: Experimental data [2]

Results: Load Response to Platform Motions

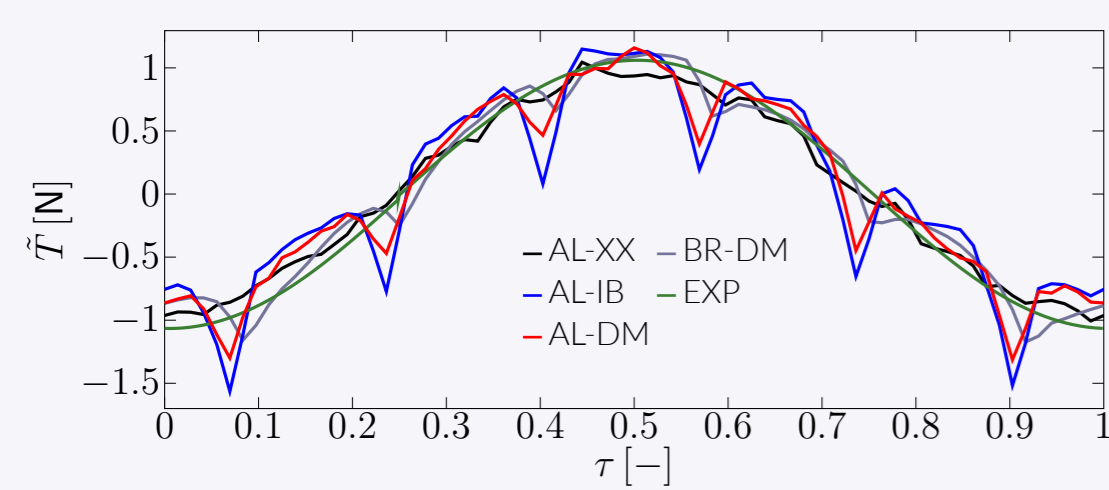


Figure 2. Coherent component of the rotor thrust under pitching motions characterised by $(f_p^*, A_p) = (1.19, 0.3^\circ)$.

- ▶ Due to a blade-mass imbalance, the EXP data was low pass filtered with a cut-off frequency below the blade-passing frequency, f_b^* .
- ▶ The rotor thrust response to platform motion frequency, ΔT_p^* , is captured with excellent accuracy. In contrast, the tower shadow effect is significantly overpredicted by the AL-IB/AL-DM configurations, likely due to non-local velocity sampling.

	\bar{T} [N]	ΔT_p^* [N]	ΔT_b^* [N]
AL-XX	35.71	0.955	0.027
AL-DM	35.76	0.965	0.207
AL-IB	35.66	0.949	0.325
BR-DM [1]	35.01	1.015	-
EXP [2]	36.19	0.957	-

Table 1. Time-averaged thrust, \bar{T} , and amplitudes of thrust oscillation at blade-passing, ΔT_b^* , and platform, ΔT_p^* , frequency for a pitching turbine with $(f_p^*, A_p) = (1.19, 0.3^\circ)$.

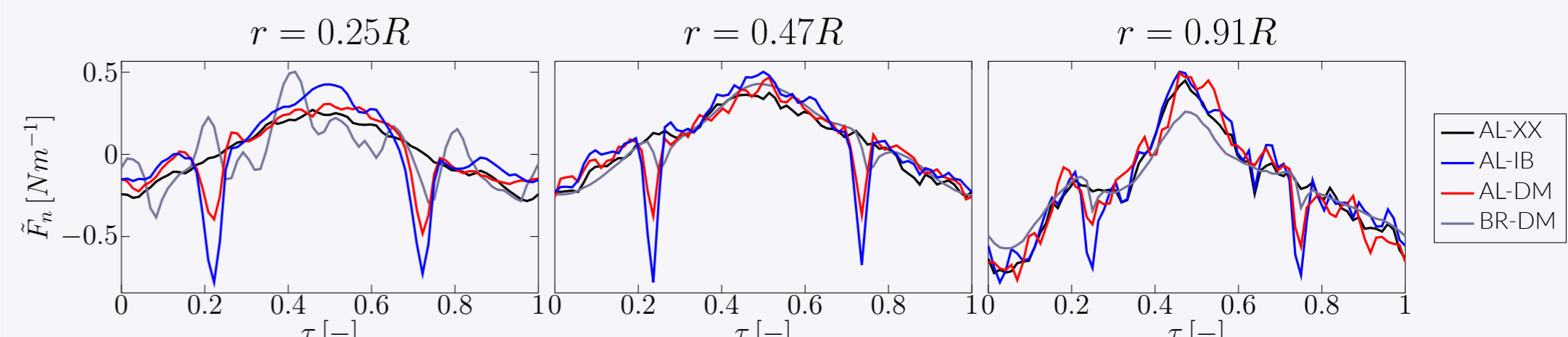


Figure 3. Coherent component of the normal force per unit blade length at three different blade sections for the blade in the vertical position at $\tau = 0$ for a pitching turbine with motions characterised by $(f_p^*, A_p) = (1.19, 0.3^\circ)$.

- ▶ As in Figure 2, the general trends are captured well however significant discrepancies are observed in the amplitude of the tower shadow effect.
- ▶ The inboard section exhibits significant deviation from the BR-DM reference data as a result of the highly 3D flow which cannot be realised by the 2D polars using by the actuator line model.

Results: Wake Response to Platform Motions

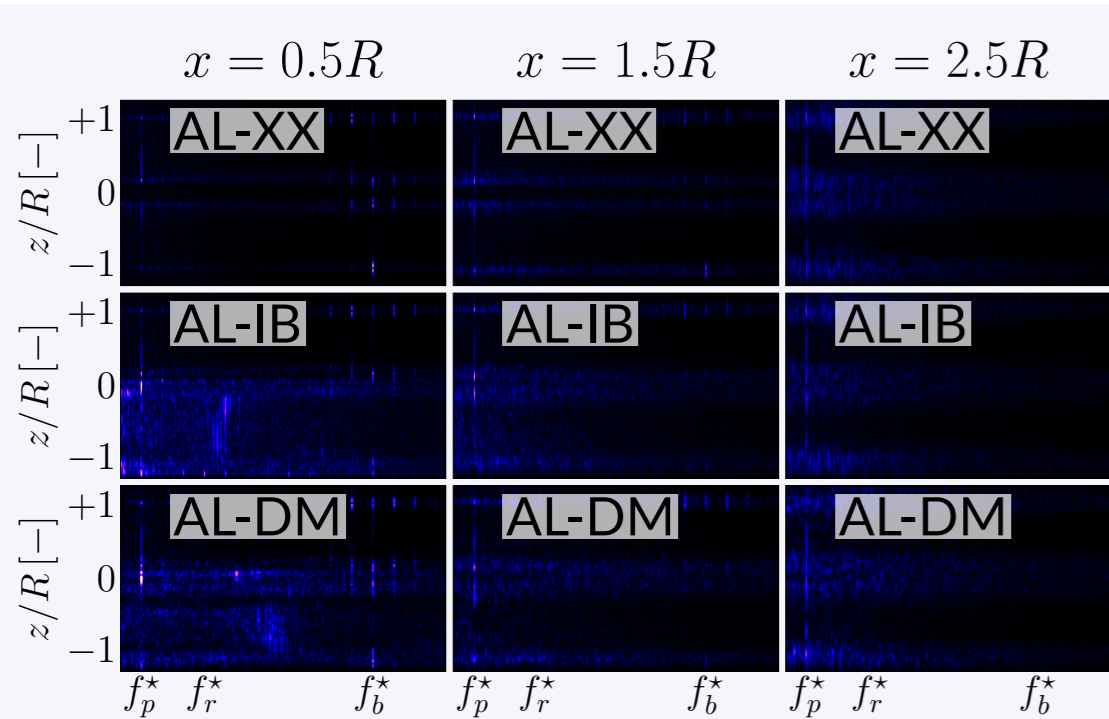


Figure 4. Wake streamwise velocity spectra as a function of the vertical distance, z , relative to the hub height at the initial rotor position for a pitching turbine with $(f_p^*, A_p) = (0.60, 1.9^\circ)$ at different downstream locations, $x = 0.5R, 1.5R, 2.5R$.

- ▶ At $r = 0.5R$, the spectra exhibit distinct peaks at the platform-motion frequency f_p^* , the blade-passing frequency f_b^* , and their associated combination tones $f_b^* \pm f_p^*$ and $f_b^* \pm 2f_p^*$.
- ▶ The tower wake generates a broadband spectra in the lower half of the wake. The characteristic frequency of this is underpredicted by the AL-IB relative to the AL-DM.
- ▶ The spurious nacelle jet produced by the AL-XX appears to suppress oscillations near the centre line.
- ▶ By $r = 2.5R$, the spectra is has broad banded structure as a result of turbulence breakdown of the near wake structures with a persistent peak at f_p^*

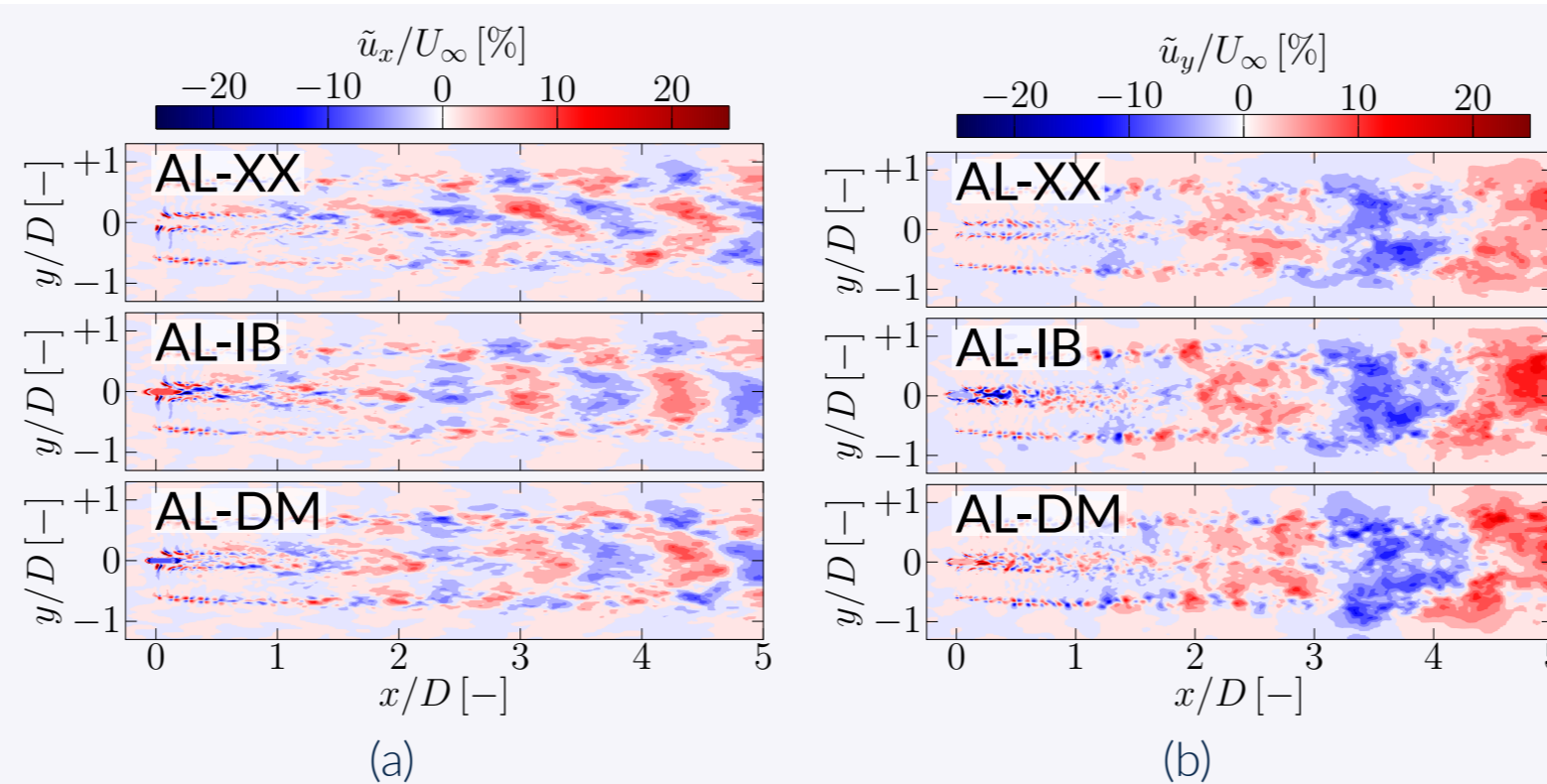


Figure 5. Coherent velocity contours at $\tau = 0.5$ and coherent standard deviation of the integrated velocity for (a,c) a pitching turbine and (b,d) a rolling turbine with $(f_p^*, A_p) = (0.60, 1.9^\circ)$ and $(0.30, 1.9^\circ)$, respectively. The planes are located at the initial hub height. The velocity component is chosen to align with the platform induced velocity.

- ▶ Platform motions generate large scale coherent structures, as can be seen in the regions of coherent velocity in Figure 5 (a) and (b).
- ▶ Figure 5 (c) and (d) demonstrate that while pitching motions show no significant increase in wake coherence as a results of the tower and nacelle model, roll-induced meandering appears to be amplified by the inclusion of the tower and nacelle model.

Results: Computational Cost

	AL-XX	AL-IB	AL-DM
Relative Cost	-	+7.5%	+365%

Table 2. Computational cost of each methodology relative to the AL-XX configuration.

- ▶ The AL-DM requires significantly more (4.33x) computational resources compared to the AL-IB method.

Conclusions

- ▶ All models reproduced platform-frequency rotor thrust in line with experiments and blade-resolved data.
- ▶ ALM strongly overpredicted tower-shadow amplitudes due to non-local velocity sampling.
- ▶ The tower generated a broad wake spectra while the inclusion of the nacelle prevented jet formation which was shown to suppress the wake spectra.
- ▶ For the motions examined, the tower and nacelle had minimal impact on pitch-induced coherent structures but amplified roll-induced wake meandering.
- ▶ AL-DM incurred a significantly higher (4.33x) computational cost compared to the AL-IB representing a major strength of the AL-IB.

References

- [1] Stefano Cioni, Francesco Papi, Francesco Balduzzi, Alessandro Fontanella, and Alessandro Bianchini. *Ocean Engineering*, 341:122746, 2025.
- [2] A. Fontanella, A. Fusetti, S. Cioni, F. Papi, S. Muggiasca, G. Persico, V. Dossena, A. Bianchini, and M. Belloni. *Wind Energy Science*, 10(7):1369–1387, 2025.
- [3] R. Poletto, T. Craft, and A. Revell. *Flow, Turbulence and Combustion*, 91(3):519–539, Oct 2013.
- [4] Justine Schluntz and Richard H. J. Willden. *Wind Energy*, 18(8):1469–1485, 2015.